Journal of Electrical and Computer Engineering Innovations

(JECEI)

SRTTU JECEI

**Research paper**

# Improving the Tracking Error Signal Extraction in IR Seeker with Stationary Wagon Wheel Reticle over all Field of View

***O. Abbas*[1]*, M.R. Arvan*[*]*, A. Mahmoudi***

*Malek-Ashtar University of Technology, Tehran, Iran.*

## Article Info

**Article History:**
Received 09 September 2017
Revised 25 February 2018
Accepted 06 May 2018

**Keywords:**
FM modulation
Field of View (FOV)
Hilbert transform
Seeker
Wagon wheel reticle

[*]Corresponding Author's Email Address: arvan@mut.ac.ir

## Extended Abstract

**Background and Objectives:** The accuracy of target position detection in IR seeker depends on the accuracy of tracking error signal (TES) extraction from seeker Field of View (FOV). The type of reticle inside the seeker determines the output modulation signal that carries the TES. In this paper, the stationary wagon wheel reticle is used, which makes the type of the output signal as FM modulation in the linear region of FOV, but the signal will be distorted by changing the radius of target image spot (TIS) and in the nonlinear region of FOV.

**Methods:** Firstly, we applied the Hilbert transform algorithm for the first time in this field and compared it with the conventional algorithm in the linear region of FOV to decrease the effect of changing the radius of TIS. Secondly, we presented a new method in the nonlinear region to extract the TES.

**Results:** The results show improvement in TES accuracy extraction in the linear and nonlinear region over the FOV for different radii of TIS.

**Conclusion:** Improving the TES extraction in all FOV will improve the ability of the missile to track the target. This extraction faces problems like existence the target in the nonlinear region of FOV and changing the radius of the TIS.

## Introduction

The IR seeker in a passive homing missile is the 'eye' of the missile and contains an optical system to view the target image. The final output of the optical system, which is the output of the IR detector, is the information signal (IS). The useful information, which is extracted from IS using the electronic unit in the seeker, is the tracking error signal (TES).

The TES will be used to direct the gyro toward the target, and the autopilot block converts TES into control signal to correct the course of the missile. So, the accuracy of measuring the amplitude and phase of this signal will be reflected directly on the accuracy of target tracking. To extract TES, we have to demodulate the IS signal. In this investigation, we used a stationary wagon wheel reticle which means that the type of modulation is FM in the linear region. We will deal with two main problems in the TES extraction as follows:

First thing is the limitation of linear region. In the wagon wheel reticle, the linear region is only 40% of FOV [1]. The linear region in the wagon wheel reticle is the region where the projection of the target at reticle plane will produce the FM modulation signal. In the IR seeker, the target may be missed before going out of the FOV because it is becoming in the nonlinear region of the FOV [2]. The efforts to extend the linear tracking field beyond the maximum point in linear region by special demodulation techniques have been unsuccessful [3].

The second problem is changing the radius of the target image spot (TIS) at the reticle plane. This changing depends on the distance between the missile and the target. When the missile approaches from the target the radius of the TIS will increase, and the IS will distort. The conventional algorithm is sensitive to this distortion.

Many papers studied and analyzed the frequency-modulation of stationary reticle and jamming such as [4], [5], without any look on the effect of the target IR image size at the accuracy of TES over FOV.

The famous conventional algorithm to demodulate FM signal is by changing it to AM modulation because it can be implemented with analog technology [6], [7].

Many algorithms can be used to demodulate FM signals such as Hilbert Transform (HT). The Hilbert transform is a fundamental operation in many different areas of science and engineering because of its close relation to causality [8]. HT is an effective tool for analysing signals. It can indicate frequency–amplitude differences with time and extract some time–frequency characteristics, so it is a good algorithm in demodulation such as in [9], [10].

In this paper, first we compare the conventional and Hilbert transform-based algorithms in the linear region of FOV. Then, we add the new method in the nonlinear region to improve the TES over all FOV.

## Stationary Reticle

The reticle systems are considered to be the classical approach in estimating the position of a target in a considered field of view and are widely used in infrared seekers [4]. The position of the target is projected on the plane of the reticle as shown in Fig. 1 [11].

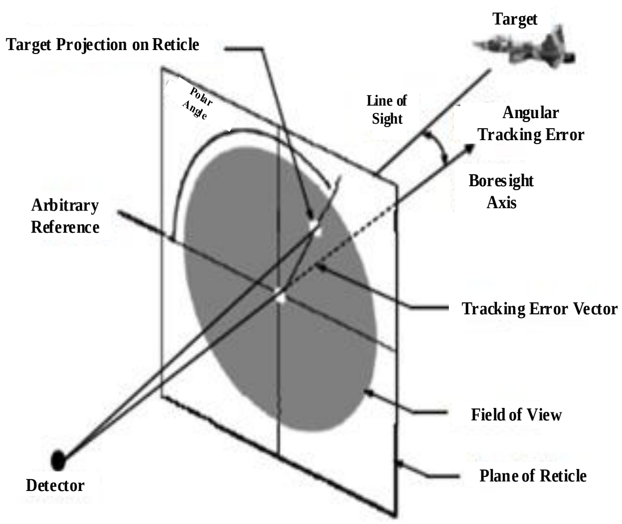


Fig. 1: Projection of tracking error at the reticle plane [11].

There are two main types of Reticle:

- The non-stationary reticle (spin-scan): The reticle rotates about an optical axis; the famous output modulation is AM modulation like sunrise reticle.
- The stationary reticle (conical-scan): The reticle is stationary and the mirror of optical system rotates off axis. It offers additional flexibility in types of modulation and offers the important feature that there is no loss of carrier for zero pointing error [3]. Herein, the famous output modulation is FM. Fig. 2 shows wagon wheel reticle with a conical scan, which will produce FM modulation. We obtained this result by using the MATLAB program in order to use it in IS generation. where, Rr is the radius of reticle; Rn is the radius of nutation circle; Rs is the radius of target image; $m_m$ is the amplitude of tracking error signal, which expresses the distance between the center of reticle and the center of nutation circle (dc); φ is the phase of tracking error signal, which expresses the phase appeared by changing the position of nutation circle center on the reticle plane; and finally, N is the number of transparent sectors.

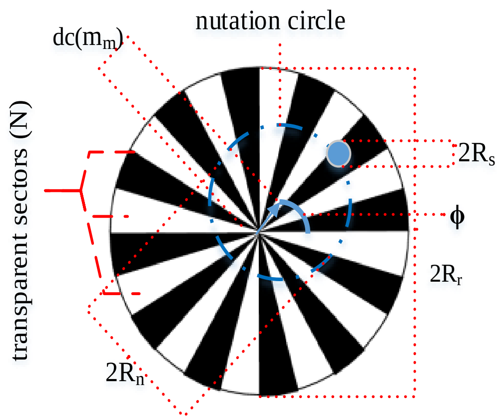


Fig. 2: Wagon wheel with a conical scan.

## Modulation

In the reticle system, the rotation of the mirror will draw a circle called nutation circle. The output of the reticle is FM signal which has the following form:

$$\begin{cases} sig = s.\sin(2\pi F_c t + \theta) & : \theta = \delta \int m(t)dt \\ \qquad m(t) = m_m \sin(2\pi F_m t + \phi) \end{cases} \tag{1}$$

Where, Sig is the information signal; Fc is the carrier frequency, which equals to N×Fm; Fm is the rotation frequency of the gyro; θ is the phase of information signal; δ is the modulation index; and s is the amplitude of the information signal. Herein, dn is the normalized dc to reticle radius (dn=dc/Rr).

Both Fig. 3 and Fig. 4 show the output of reticle for a different tracking error where in Fig. 3, dn=0.078 and φ=135 , and in Fig. 4, dn=0.156 and φ=45. N=12, Fm=80Hz (Fc=12×80=960 Hz) are similar for both figures.

## Demodulation in Linear Region of FOV

*A. Conventional Demodulation Algorithm*

Fig. 5 shows the block diagram of the conventional FM demodulation algorithm. First, we transfer the demodulation from FM to AM by differentiating the FM signal and consequently apply AM demodulation. The AM demodulation contains the envelope detection and bandpass filtering, where the center frequency is Fm.

Fig. 6 shows the outputs of the demodulation algorithm for the information signals from Fig. 3 and Fig. 4.

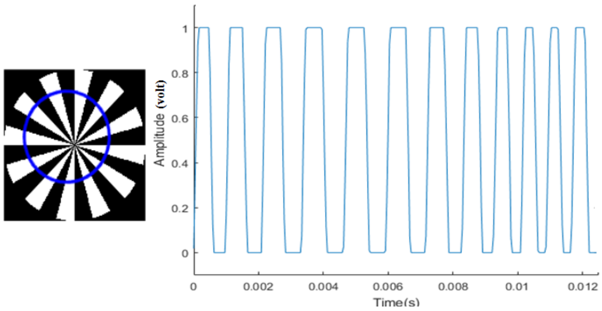


Fig. 3: The output of reticle for dn=0.078 and φ=135°.

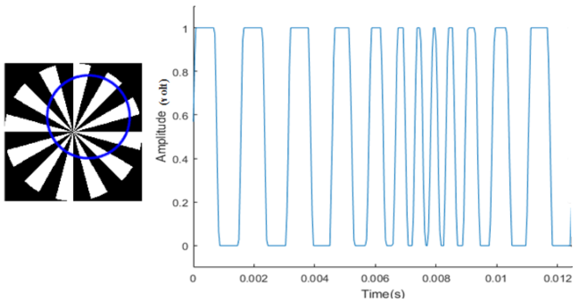


Fig. 4: The output of reticle for dn=0.156 and φ=45°.

*B. Hilbert Transform Algorithm*

In signal processing, using the analytical signal instead of the real-valued signal is very useful in many applications such as demodulation. The real and imaginary parts of an analytical signal are related to each other by a Hilbert transform. The HT solves a typical demodulation problem, giving the amplitude (envelope) and instantaneous frequency of a measured signal. For continuous signal x(t), the HT is defined as [12]:

$$H[x(t)] = x(t) * \frac{1}{\pi t} = \frac{1}{\pi} \int_{-\infty}^{\infty} \frac{x(\tau)}{t-\tau} d\tau \qquad (2)$$

In the frequency domain:

$$H[X(f)] = X(f)[-j \operatorname{sgn}(f)] \qquad (3)$$

The analytical signal y(t) of x(t) can be written in the time domain as:

$$y(t) = x(t) + jH[x(t)] = A(t) e^{j\phi(t)} \qquad (4)$$

where:

$$\begin{cases} A(t) = |y(t)| = \sqrt{x^2(t) + H^2[x(t)]} \\ \phi(t) = \arg[y(t)] \end{cases} \qquad (5)$$

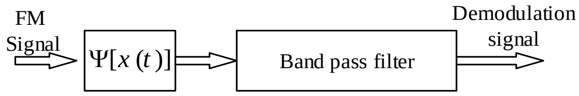


Fig. 5: Conventional FM demodulation algorithm.

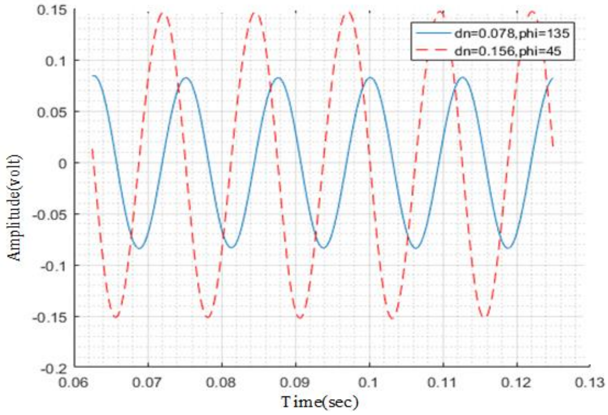


Fig. 6: The output of FM demodulation algorithm for the signals from Fig. 3 and Fig. 4.

The instantaneous frequency of signal can be computed as:

$$f(t) = \frac{1}{2\pi} \frac{d\phi}{dt} \qquad (6)$$

The analytical signal in the frequency domain can be written as:

$$Y(f) = \begin{cases} X(0) & for \quad f = 0 \\ 2X(f) & for \quad f > 0 \\ 0 & for \quad f < 0 \end{cases} \qquad (7)$$

Fig. 7 shows the block diagram of this algorithm.

## Demodulation in Nonlinear Region of FOV

The signal modulation will change from FM modulation to AM/FM modulation when the distance between center of nutation circle and reticle distance become larger than (Rr-Rn). Fig. 8 illustrates a typical static gain curve obtained by the conventional signal processing [1]. In this paper we selected Rn=0.6*Rr, which means the linear region equal 40% of FOV (the FOV over reticle plane with radius Rr).

*C. Select the Region of FOV*

Before applying any algorithm we have to select the region of FOV is it linear or nonlinear?

In the linear region the type of modulation is FM and the DC signal is constant, but in nonlinear region the type of modulation is AM/FM modulation because the spot light of target will pass over the different width of transparent sector. When the amplitude of AM signals increase the DC signal will decrease. Fig. 9 shows this different. The DC signal will decrease when the distance dn becomes larger than 0.4 of FOV ((Rr-Rn/Rr)=0.4).

So we select the region depending on the difference between DC amplitude and the amplitude of AM signal.

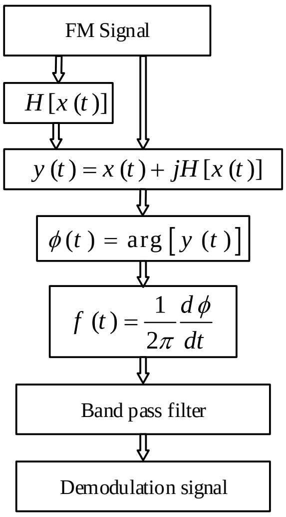


Fig. 7: The block diagram of FM demodulation using Hilbert transform.

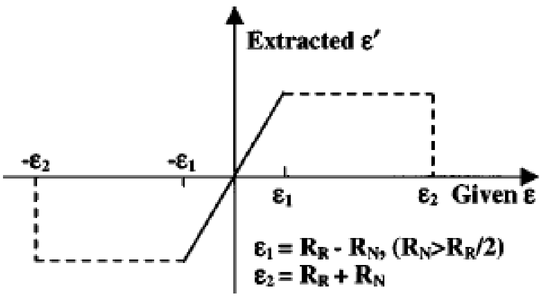


Fig. 8: Typical static gain curve obtained by the conventional algorithm; the solid line represents the linear region and the dotted line represents the nonlinear region [1].

*D. Nonlinear Algorithm.*

The changing in amplitude of the detector signal will produce “gap” because of AM signal. In the real cases, the signal is a pseudo AM instead of an AM. So, if we apply the AM demodulation algorithm, the phase will not be stable over dn. For this reason, we use this gap to calculate the phase.

Fig. 10 shows the different signals for constant dn and different phases.

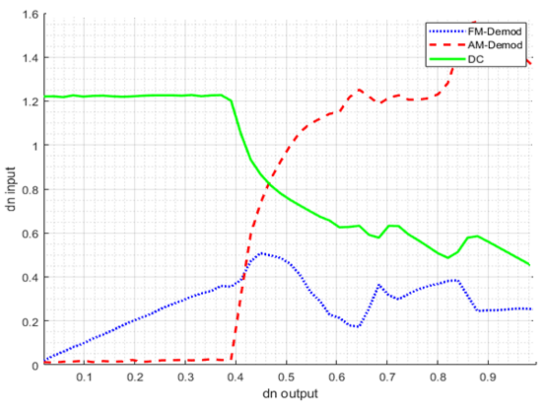


Fig. 9: The DC, AM and FM demodulated signals.

The algorithm to calculate the phase has these steps:

- Detect the peaks of signal.
- Plot pulse signal for low peak.
- Determine the delay of pulse.
- Calculate the phase depending on this delay.

Amplitude calculation: the DC value will decrease linearity, so we use the inverse of DC value with gain.

Fig. 11 shows the block diagram for linear and nonlinear algorithms.

## The Simulation Result

In this simulation we define these values: Rr=256 pixel, Rn=0.6*Rr, N=12, Fm=80Hz. The linear region of FOV is [0 0.4] and the nonlinear region of FOV is [0.41].

In all figures the part (a) shows the phase output, and part (b) shows the normalized amplitude output of tracking error via normalized amplitude input.

*E. Linear Region*

We change the normalized radius of target image spot and select three scenarios as shown in Table 1. The results for scenario1, 2, and 3 are shown in Fig. 12-14, respectively.

We define in these figures:

- The output of a conventional demodulation algorithm.
- The output of Hilbert transform algorithm.

Table 1: Scenarios of simulation where phase=45$^{o}$ and dn belongs [0 0.4]

| Scenario | The normalized radius of target image spot (Rsn) |
|---|---|
| 1 | 0.02 |
| 2 | 0.04 |
| 3 | 0.06 |

These figures show that the HT algorithm provides more accuracy than the conventional algorithm.

For more comparison, we selected different phases. Table 2 and Table 3 present the mean square error in the phase and normalized amplitude, respectively.

There is a similarity between the four quarters of reticle so we select the first quarter and uses different phases in it to be more confident about our results.

We can summarize the results as follows:

- HT algorithm: This algorithm has a high performance in detecting phase and amplitude. The effect of target image change didn’t appear.

Conventional algorithm: It has a good performance in detecting phase when the radius of the target image spot is changing, but in amplitude the performance is low.

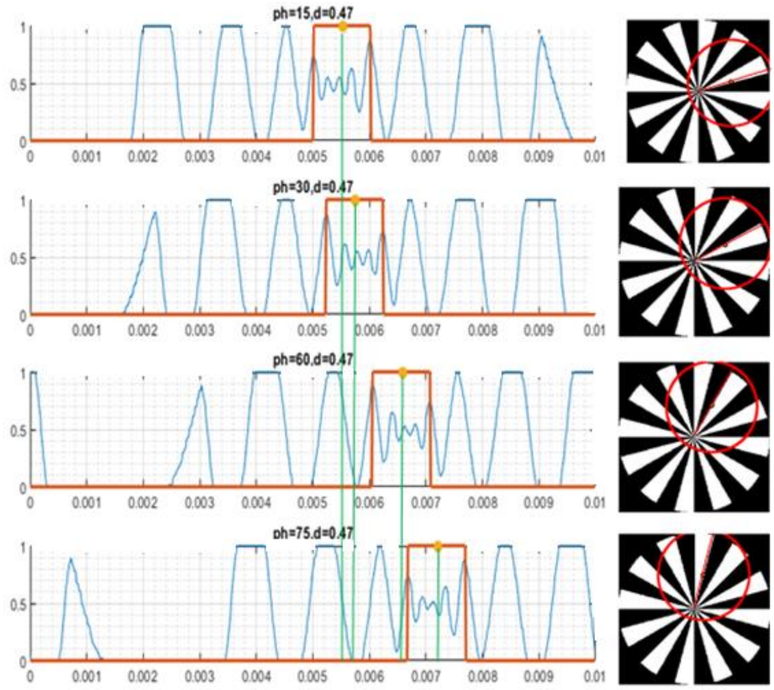


Fig. 10: The gap position moving for different phase and constant dn.

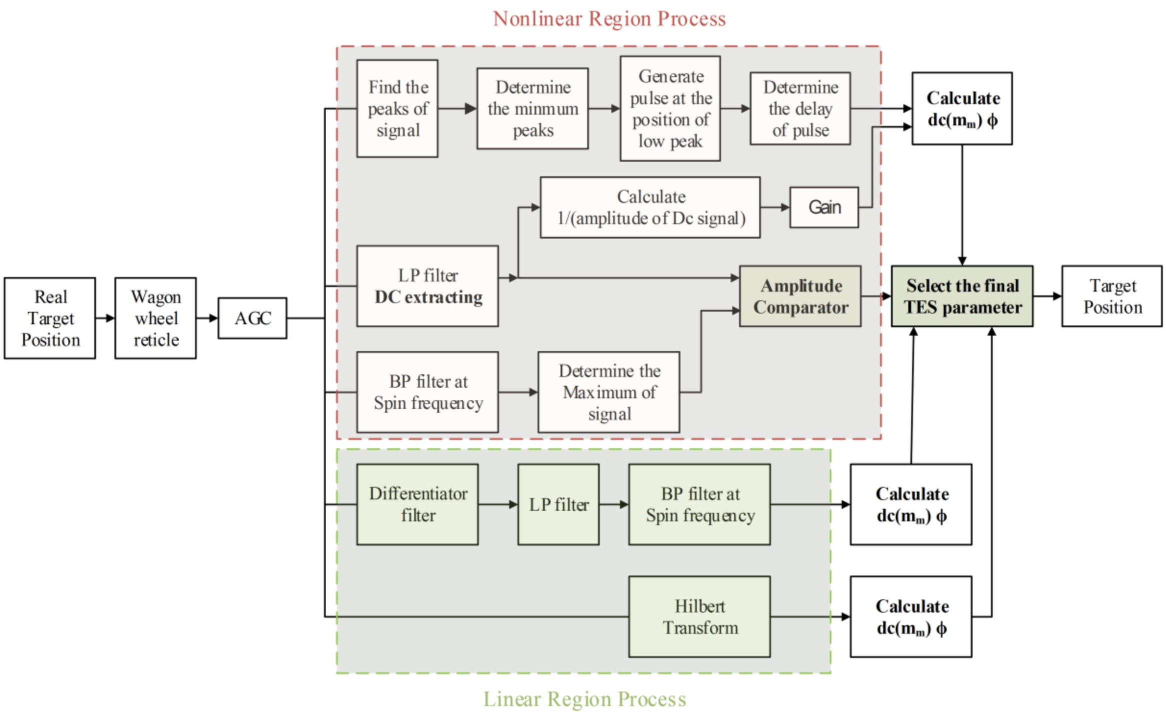


Fig. 11: The Block diagram of linear and nonlinear algorithms.

*F. Total FOV*

From the previous result, we select the Hilbert transform-based algorithm for linear region. For nonlinear region, we apply the new proposed algorithm. We select three scenarios as shown in Table 4.

The results for scenarios 4, 5, and 6 are shown in Figs. 15-17, respectively.

For seeing the more details, we selected different phases. Table 5 and Table 6 present the root of mean square error in the phase and normalized amplitude, respectively. We divided the nonlinear region to two regions:

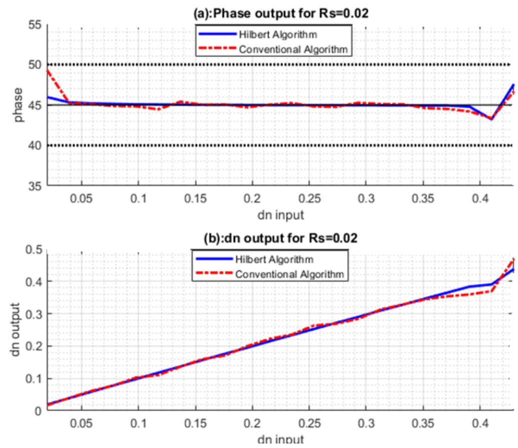


Fig. 12: The results of scenario 1: (a) Phase output, (b) dn output.

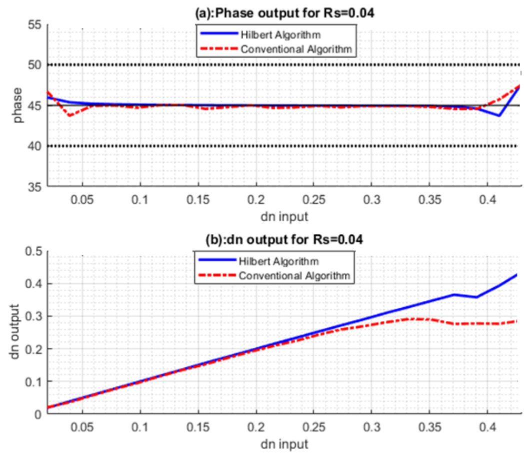


Fig. 13: The results of scenario 2: (a) Phase output, (b) dn output.

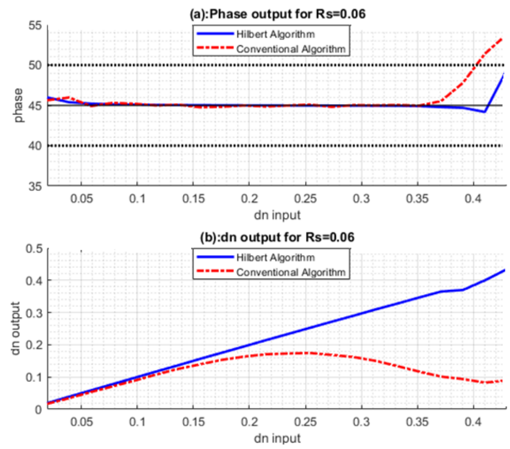


Fig. 14: The results of scenario 3: (a) Phase output, (b) dn output.

- Region 1 (dn in [0.4 0.7]): In the new algorithm, the maximum error in phase for different Rsn is 3.47°, where in the conventional algorithm is 17.29°. It means that the error in amplitude for the conventional algorithm is not acceptable. But, in the new method, the maximum error is 0.04, which is acceptable. Region 2 (dn in [0.7 1]): In the new algorithm, the maximum error in phase for different Rsn is 8.18°, where in the conventional algorithm it is 18.15°. It means that the error in amplitude for conventional algorithm is not acceptable. But, in the new method, the maximum error is 0.1, which is acceptable.

Table 2: The mean square error of phase in linear region

| phase | Rsn | Conventional algorithm (degree)$^2$ | Hilbert transform (degree)$^2$ |
|---|---|---|---|
| | 0.02 | 0.29 | 0.11 |
| 0 | 0.04 | 0.48 | 0.13 |
| | 0.06 | 1.12 | 0.12 |
| | 0.02 | 3 | 0.48 |
| 30 | 0.04 | 1.2 | 0.47 |
| | 0.06 | 5.1 | 0.9 |
| | 0.02 | 1.18 | 0.49 |
| 45 | 0.04 | 0.58 | 0.48 |
| | 0.06 | 5.8 | 0.96 |
| | 0.02 | 14 | 0.2 |
| 60 | 0.04 | 0.6 | 0.22 |
| | 0.06 | 0.8 | 0.21` |
| | 0.02 | 7.3 | 0.18 |
| 75 | 0.04 | 1.1 | 0.2 |
| | 0.06 | 0.69 | 0.21 |

Table 3: The mean square error of normalized amplitude in linear region

| phase | Rsn | Conventional algorithm ($\times10^{-4}$) | Hilbert transform ($\times10^{-4}$) |
|---|---|---|---|
| | 0.02 | 8 | 0.7 |
| 0 | 0.04 | 14 | 0.6 |
| | 0.06 | 162 | 0.6 |
| | 0.02 | 1 | 0.3 |
| 30 | 0.04 | 31 | 0.3 |
| | 0.06 | 247 | 0.9 |
| | 0.02 | 2 | 0.3 |
| 45 | 0.04 | 30 | 0.3 |
| | 0.06 | 248 | 0.4 |
| | 0.02 | 0.7 | 0.7 |
| 60 | 0.04 | 13 | 0.7 |
| | 0.06 | 160 | 0.7` |
| | 0.02 | 1 | 0.6 |
| 75 | 0.04 | 14 | 0.6 |
| | 0.06 | 159 | 0.6 |

Table 4: Scenarios of simulation where phase=45° and dn in [0 1]

| Scenario | The normalized radius of target image spot (Rsn) |
|---|---|
| 4 | 0.02 |
| 5 | 0.04 |
| 6 | 0.06 |

## Conclusion

Improving the tracking error signal (TES) extraction in all FOV will improve the ability of the missile to track the target. This extraction faces problems like existence the target in the nonlinear region of FOV and changing the radius of the target image spot (TIS). There are no classic algorithms to extract the tracking error signal in the nonlinear region which is larger than the linear region, and the conventional algorithm has not acceptable ability to accept changing the radius of TIS in the linear region.

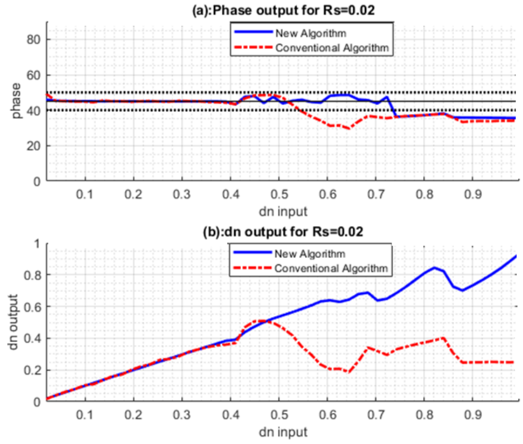


Fig. 15: The results of scenario 4: (a) Phase output, (b) dn output.

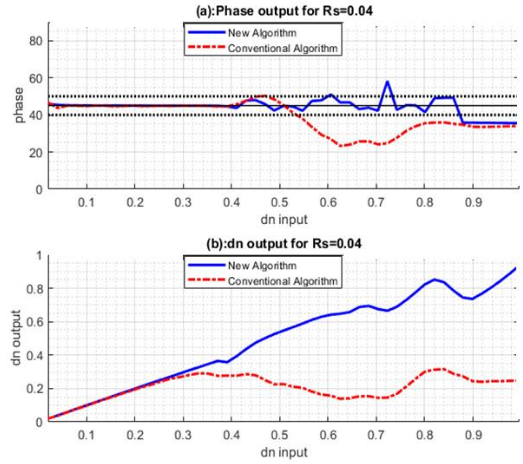


Fig. 16: The results of scenario 5: (a) Phase output, (b) dn output.

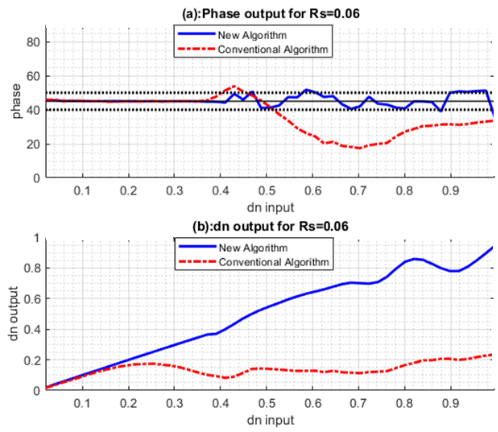


Fig. 17: The results of scenario 6: (a) Phase output, (b) dn output.

Table 5: the root mean square error of phase in nonlinear region

| phase | Rsn | Conventional algorithm (degree) dn nonlinear region | | New algorithm (degree) dn nonlinear region | |
|---|---|---|---|---|---|
| | | [0.4 0.7] | [0.7 1] | [0.4 0.7] | [0.7 1] |
| | 0.02 | 8.42 | 9.5 | 1.87 | 7.9 |
| 0 | 0.04 | 13.05 | 13.3 | 2.5 | 6.2 |
| | 0.06 | 16.80 | 17.4 | 3.47 | 4.6 |
| | 0.02 | 8.64 | 9.4 | 1.9 | 7.8 |
| 30 | 0.04 | 13.17 | 12.3 | 3.15 | 6.2 |
| | 0.06 | 16.85 | 17.7 | 3.37 | 4.4 |
| | 0.02 | 8.51 | 9.70 | 2.03 | 8.18 |
| 45 | 0.04 | 13.52 | 12.92 | 2.53 | 7.32 |
| | 0.06 | 17.22 | 18.15 | 3.41 | 4.62 |
| | 0.02 | 8.76 | 9.50 | 2.44 | 8.00 |
| 60 | 0.04 | 13.42 | 12.55 | 3.10 | 6.67 |
| | 0.06 | 17.29 | 17.85 | 3.10 | 4.60 |
| | 0.02 | 8.70 | 9.65 | 1.71 | 8.10 |
| 75 | 0.04 | 13.01 | 12.66 | 2.41 | 6.53 |
| | 0.06 | 16.85 | 18.11 | 3.33 | 6.08 |

Our simulation results showed an improved accuracy of TES in all FOV. Firstly, in the linear region by using the Hilbert transform algorithm which decreases the effect of changing the target image spot and the improvement was more than 100%. Secondly, in the nonlinear region, the error in phase and amplitude of TES was not acceptable by using the conventional algorithm, but by using the new method the error in phase and amplitude is acceptable for this problem. The next research work related to this work is studying the effect of noise at the TES extraction, which is in the progress.

Table 6: The root mean square error of normalized amplitude in nonlinear region

| phase | Rsn | Conventional algorithm (degree) dn nonlinear region | | New algorithm (degree) dn nonlinear region | |
|---|---|---|---|---|---|
| | | [0.4 0.7] | [0.7 1] | [0.4 0.7] | [0.7 1] |
| | 0.02 | 0.27 | 0.54 | 0.035 | 0.10 |
| 0 | 0.04 | 0.38 | 0.60 | 0.035 | 0.09 |
| | 0.06 | 0.45 | 0.66 | 0.039 | 0.07 |
| | 0.02 | 0.27 | 0.55 | 0.033 | 0.10 |
| 30 | 0.04 | 0.37 | 0.60 | 0.035 | 0.09 |
| | 0.06 | 0.44 | 0.67 | 0.04 | 0.08 |
| | 0.02 | 0.28 | 0.56 | 0.032 | 0.10 |
| 45 | 0.04 | 0.38 | 0.61 | 0.031 | 0.08 |
| | 0.06 | 0.44 | 0.67 | 0.034 | 0.07 |
| | 0.02 | 0.27 | 0.55 | 0.032 | 0.09 |
| 60 | 0.04 | 0.38 | 0.60 | 0.030 | 0.09 |
| | 0.06 | 0.45 | 0.67 | 0.031 | 0.07 |
| | 0.02 | 0.28 | 0.56 | 0.029 | 0.09 |
| 75 | 0.04 | 0.38 | 0.61 | 0.028 | 0.08 |
| | 0.06 | 0.44 | 0.67 | 0.032 | 0.07 |

## References


[1] J. Oh, K. Doo, S. Jahng, D. Seo, J. S. Choi, “Novel adaptive digital signal processing algorithm for a stationary reticle seeker,” Optical Engineering, 39(10): 2797-2804, 2000.

[2] A. Yrfanean, M. Mosavi, A. Mohammadi, S. A. Yasin, “Improving the target position detection in the crossed array detectors seeker by categorizing the FOV up to the pulses distribution,” International Journal of Computer Applications, 72(4): 28-36, 2013.

[3] G. Olsson, “Selected papers on reticles and their applications,” Society of Photo-Optical Instrumentation Engineers (SPIE), 1999.

[4] G. Olsson, “Simulation of reticle seekers by means of an image processing system,” Optical Engineering, 33(3): 730-737, 1994.

[5] T. M. Malatji, C. J. Willers, M. S. Willers, “Propagation of a jam code signal in the conical-scan seeker processor,” in Proc. International Conference on Intelligent and Innovative Computing Applications (ICONIC): 1-6, 2018.

[6] J. Jackman, M. Richardson, B. Butters, R. Walmsley, "Modelling a man-portable air-defence ( MANPAD) system with a conical scan two-colour infrared (IR) seeker," in Proc. Technologies for Optical Countermeasures VIII, 8187, p. 81870S, 2011.

[7] T. M. Malatji, W. P. du Plessis, C. J. Willers, “Analysis of the jam signal effect against the conical-scan seeker,” Optical Engineering, 58(2): 025101, 2019.

[8] H. Boche, V. Pohl, “Investigations on the approximability and computability of the Hilbert transform with applications,” Applied and Computational Harmonic Analysis.

[9] S. Qin, Y. Qin, Y. Mao, “Accurate instantaneous frequency estimation with iterated Hilbert transform and its application,” in Proc. 7th WSEAS International Conference on Signal Processing, Robotics and Automation: 165-170, 2008.

[10] Z. X. Hu, W. X. Ren, Z. C. Wang, Y. L. Jing, X. Yang, “A generalized demodulation and Hilbert transform based signal decomposition method,” Shock and Vibration,: 1-12, 2017.

[11] J. Strickland, Missile Flight Simulation. Lulu. com, 2015.

[12] K. Li, J. Tian, C. Li, M. Liu, C. Yang, G. Zhang, “The detection of low frequency oscillation based on the Hilbert-Huang transform method," in Proc. China International Conference on Electricity Distribution (CICED)): 1376-1379, 2018.


## Biographies


**Osama Abbas** received his B.Sc. degree in Communication Engineering from Higher Institute for Applied Science and Technology (HIAST) Damascus, Syria, in 2002 and the M.Sc. degree in Communication Systems from Malek Ashtar University of Technology (MUT), Tehran, Iran, in 2011. He is currently working toward a Ph.D. in Control Science and Engineering, Malek Ashtar University of Technology. His area of interests is Signal processing, Estimation, Guidance and Control.

**Mohammad Reza Arvan** received his B.Sc. in Electronics from the Sharif University of Technology, Tehran, Iran, in 1992 and M.Sc. degree in Control systems from University of Tehran, Iran, in 1995, and his Ph.D. degree in Control systems from K. N. Toosi University of Technology, Tehran, Iran, in 2007. He is an associate professor at Malek Ashter University of Technology. His current research interests include Control Engineering, Estimation, Modeling and Simulation, Guidance and Control.

**Ali Mahmoudi** received his B.Sc. in Electrical Engineering from Sharif University of Technology, Iran, in 1991 and his M.Sc. and Ph.D. from the University of Tarbiat-Modares, Iran, in 1994 and 2000, respectively. Currently, he is an assistant professor in the Department of Electrical Engineering at Malek-Ashtar University of Technology, Tehran, Iran. His research involves image processing and electro-optical systems.





**How to cite this paper:**

O. Abbas, M. R. Arvan, A. Mahmoudi, “Improving the tracking error signal extraction in IR seeker with stationary wagon wheel reticle over all field of view,” Journal of Electrical and Computer Engineering Innovations, 6(2): 151-158, 2018.

**DOI:** 10.22061/JECEI.2019.5062.187

**URL:** http://jecei.sru.ac.ir/article_1098.html